Optoelectronic Oscillator incorporating Hollow Core Photonic Bandgap Fiber

U.S. Mutugala[1,*], J. Kim[1,2], T.D. Bradley[1], N.V. Wheeler[1], S.R. Sandoghchi[1], J.R. Hayes[1], E. Numkam Fokoua[1], F. Poletti[1], M.N. Petrovich[1], D.J. Richardson[1], and R. Slavík[1]

[1]*Optoelectronics Research Centre, University of Southampton, Southampton, SO17 1BJ, UK*
[2]*Currently with Optical network research group, Electronics and Telecommunications Research Institute, 218 Gajeong-ro, Yuseong-gu, Daejeon, 34129, Korea*
**Corresponding author: U.S.Mutugala@soton.ac.uk*

Received XX Month XXXX; revised XX Month, XXXX; accepted XX Month XXXX; posted XX Month XXXX (Doc. ID XXXXX); published XX Month XXXX

We demonstrate the first Optoelectronic oscillator that uses Hollow-Core Photonic Bandgap Fiber (HC-PBGF) as a delay element of a sufficient length to allow for low-noise operation. We show experimentally that HC-PBGF can improve the temperature stability of the oscillator by a factor of more than 15 as compared to standard optical fiber. We also measured the oscillator's phase noise, allowing evaluation of the suitability of HC-PBGF for this application. Additionally this work also provides the first characterization of the temperature stability of a long-length (>800 m in our study) of low-thermal sensitivity (2 ps/km/K) HC-PBGF wound on a spool.

OCIS codes: *(250.0250) Optoelectronics; (060.4005) Microstructured fibers; (060.2400) Fiber properties.*

http://doi.org/XXXXXXXXXXXX

High quality microwave (>1 GHz) sources are an absolute necessity in many fields of science and technology including metrology, radio astronomy, radar, and communications. In these applications, the stability and spectral purity of the microwave source are the key parameters of interest. It is challenging however to obtain high levels of spectral purity in conventional electrical microwave generators in which frequency multiplication of a radio-frequency (RF) oscillator (e.g., quartz, which oscillates at tens of kHz to hundreds of MHz) is typically employed. This is mainly because the frequency multiplication process also multiplies the phase noise (thus degrading spectral purity) by 20logN (on a dB scale), where N is the multiplicative factor [1].

An alternative route is to directly obtain high-frequency (>10 GHz) microwave signals without multiplication with the help of photonics, e.g., using an Optoelectronic Oscillator (OEO) [2]. The OEO, first demonstrated by Yao and Maleki [2], has phase noise that is independent of the oscillating frequency and can operate up to frequencies of tens of GHz without compromising the spectral purity. These unique properties have made OEOs extremely popular within the scientific community [1], with OEOs recently becoming available commercially (e.g., from OEwaves Inc., USA).

OEOs with various architectures [2-8] have been proposed and demonstrated. The key components of an OEO are: a light source, an optical modulator, an optical delay element, a photodetector, and a filter enabling single-frequency oscillation. Out of these, the optical delay element is the critical component that differentiates an OEO from a conventional microwave generator as it can introduce a large delay (the phase noise typically decreases quadratically with the loop delay [2]), while keeping the round-trip loss (and thus also noise generated by any amplifiers within the loop) very low. Micro resonators [7], fiber-ring resonators [8], and optical fibers [2-6] have all been reported as delay elements in OEOs. Out of these, optical fibers are the most widely used as they are readily available in kilometer scale lengths and can easily be integrated into OEO setups. Phase noise values as low as -163 dBc/Hz at 6 kHz offset frequency have been reported when a16-km long optical fiber was used as the delay element [9].

Unfortunately, the propagation time of light through a standard optical fiber is susceptible to ambient temperature variations, causing the OEO loop delay to be dependent on the temperature. As the OEO oscillating frequency depends on the loop delay, temperature variations lead to thermally induced frequency drifts in the generated microwave signals. Techniques such as temperature stabilization of the OEO components [10], or locking of the OEO frequency to an external optical (optical comb) [11] or a microwave reference [12] have been reported to mitigate this issue.

Here, we demonstrate the benefits of using an OEO optical delay element made of a fiber with significantly lower thermal sensitivity than that of standard single mode optical fiber. We use Hollow-Core Photonic Bandgap Fiber (HC-PBGF) which was recently demonstrated to provide an 18.5 times lower sensitivity in the

introduced delay due to temperarute drift as compared to standard optical fiber [13]. Although the suitability of using HC-PBGF in OEOs has already been briefly discussed in the literature [14-16], the published reports up to now are limited to experimental demonstrations with HC-PBGF lengths of up to just a few tens of metres, which cannot support an OEO with sufficiently low noise (e.g. comparable to, or below, that of commercially-available microwave instruments). Longer lengths of HC-PBGF are already reported to have a positive effect on the thermal sensitivity of fiber optic gyroscopes (235-m HC-PBGF length reported in [17]). Here, we use an 860 m long HC-PBGF delay element in an OEO and evaluate it for the first time in terms of temperature induced frequency drift, compare it with an OEO that uses standard optical fibre as a delay element, and show phase noise characteristics providing a clear demonstration of the suitability of such fiber for this application .

The thermal sensitivity of an optical fiber is characterized by the Temperature Coefficient of Delay (TCD). It is determined by the thermal dependance of the group index of the fiber and the thermal dependence of the length of the fiber, and can be expressed as [13]:

$$\mathrm{TCD} = \frac{1}{L}\frac{d\tau}{dT} = \frac{n_g}{Lc}\frac{dL}{dT} + \frac{1}{c}\frac{dn_g}{dT} \qquad (1)$$

where τ is the propagation time through the fiber, L is the fiber length, c is the speed of light in vacuum, n_g is the fiber mode group index, and T is the temperature. The first term on the right hand side of Eq. 1 describes temperature-induced fiber elongation and the second term the temperature-induced group index change. For fibers made of silica a TCD of 40 ps/km/K was reported, with the temperature-induced group index change (that is mainly caused by the silica glass thermo-optic effect) responsible for 38 ps/km/K and temperature-induced elongation responsible for only 2 ps/km/K [18]. The significantly lower TCD of HC-PBGFs [13] comes from the fact that the core is formed by an air-filled hole (as shown in Fig. 1a), which has a negligible thermo-optic coefficient. As more than 99.8% of light can propagate in the air core [19], the temperature-induced group index change is strongly reduced in HC-PBGF as compared to solid core fibers [13]. Although promising, current state-of-the art HC-PBGFs still suffer from significantly higher losses than those of solid core fibers (lowest losses reported to be 1.2 dB/km [20]), which is mainly caused by scattering. HC-PBGFs are also not strictly single-mode. The energy carried by higher-order modes or energy coupled from these modes back to the fundamental mode at the fiber output causes undesired multi-path interference. This can be minimized by optimizing the launch and output coupling conditions, making the light propagation through the HC-PBGF effectively single-mode. Any residual multi-path interference (due to, e.g., imperfect fiber launch and scattering) results in intensity noise of the light propagating through the HC-PBGFs [21], which is subsequently converted into phase noise in the OEO loop [22]. Thus, it is essential to measure the phase noise of the HC-PBGF-based OEO to evaluate the level at which the imperfectly-suppressed multi-path interference degrades the OEO performance.

The 10 GHz single-loop OEO we built for our demonstration is shown in Fig. 1b. The delay element consists of an 860 m long HC-PBGF which had a 19-cell core design [23] with a core diameter of 29.5 µm and an insertion loss of 7 dB (a cross-sectional Scanning Electron Microscope (SEM) image of the HC-PBGF is shown in Fig. 1a). The HC-PBGF was spliced to standard fiber pigtails, resulting in a total loss of 15 dB. Splicing HC-PBGFS to conventional single mode fibers is challenging and can lead to high insertion losses as in our case, due to high mode field diameter mismatch and heat induced deformation of the microstructure of the HC-PBGF. However, splicing strategies are being developed which can be used to reduce the splice loss to ~ 0.5 dB per splice. [24]. The delay induced by the HC-PBGF fiber was 2.88 µs (n_g =1.003 [19]). For comparison, we used a length of standard optical fiber in the OEO. To obtain identical delay, 588 m of standard fiber (with an n_g of 1.468) would be needed. The nearest length we had in the laboratory was 500 m (Corning SMF-28e+, n_g =1.468 [25], referred to here as 'standard fiber'), which provided a slightly smaller delay of 2.45 µs. Both fibers (standard and HC-PBGF) were spooled on industry standard 16-cm diameter fiber spools. In the OEO setup, light from a continuous wave (CW) laser operating at 1550 nm was sent through a $LiNbO_3$ Mach-Zehnder modulator (MZM). Its output was amplified by a home-built Erbium doped fiber amplifier (EDFA), which contained a 10 m long Erbium doped fiber. This EDFA was needed in order to compensate for the HC-PBGF loss. The amplified signal was passed through a polarization controller before launching into the fiber delay element since HC-PBGF-to-standard fiber pigtail splices suffered from a slight polarization-dependent loss (which we measured to be ~0.75 dB). A high-speed photodiode (PD) was placed after the delay element, converting the optical signal into an electrical signal. To obtain the same optical power level at the PD for both fiber delay elements, an optical attenuator was inserted behind the standard fiber. The electrical signal at the output of the PD was then amplified (by a low-noise RF amplifier with 17 dB gain), filtered (by a 10 GHz electrical bandpass filter with 8 MHz 3-dB bandwidth), and was then amplified again (by a high power RF amplifier with 37 dB gain) before splitting it between two outputs. One output served as the OEO output and the other was fed back into the MZM, closing the OEO loop. The MZM bias point was kept in quadrature using a feedback loop [26].

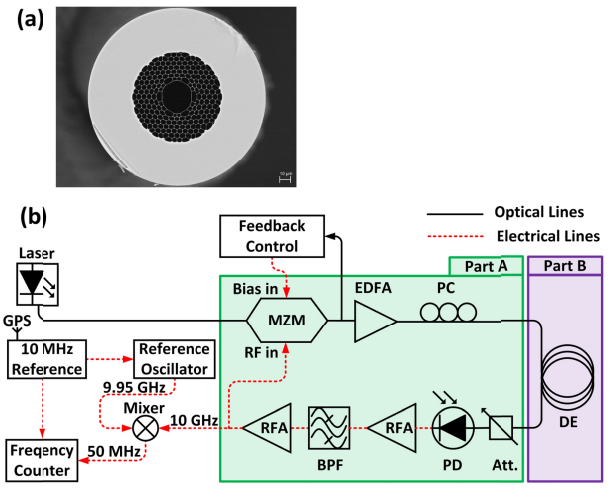

Fig. 1. (a) Cross sectional Scanning Electron Microscope (SEM) image of the HC-PBGF used, (b) experimental OEO setup. MZM: Mach-Zehnder Modulator, PC: Polarization controller, DE: Delay element, PD: Photodiode, RFA: RF amplifier, EDFA: Erbium-doped fiber amplifier, Att.: Attenuator, BPF: Band-pass filter, GPS: Global positioning system.

The drift of the OEO carrier frequency (10 GHz) was measured using a frequency counter (model: FXM50, Menlo Systems GmbH, Germany) after down-converting the signal to 50 MHz by mixing it with a 9.95 GHz reference signal. The down converting signal (9.95 GHz) was obtained by detecting the 40th RF beat tone of a 248.75 MHz optical frequency comb (model: FC1500, Menlo Systems GmbH, Germany). Both the frequency counter and the repetition rate of the optical frequency comb were locked to a high stability, GPS (Global Positioning System) synchronized, 10 MHz oscillator (model: RefGen 10491, TimeTech GmbH, Germany).

First, we measured the performance of the OEO by exposing it entirely (i.e. all of the constituent components shown in Part A and Part B in Fig. 1b) to ambient temperature variations. As shown in Fig. 2a, due to the switching on and off of the laboratory air-conditioning unit, there was a periodic ambient temperature variation of 2 °C (measured with a thermistor placed between Part A and Part B (Fig. 1b) of the setup). Under these temperature variations, the OEO carrier frequency varied on average by 18 kHz and 120 kHz for the HC- PBGF and the standard fiber based OEOs, respectively (Fig. 2b). It should be noted that even though the OEO loop delay is mainly determined by the delay element, the optical and electronic components of the OEO shown inside Part A also contribute to the total loop delay (we measured this delay to be around 250 ns). Under these conditions, the HC-PBGF-based OEO frequency drift was 6.7 times lower than that of the standard fiber-based OEO. This result demonstrates that a significant frequency stability improvement is obtained with the HC-PBGF delay element when the entire OEO is subject to temperature variations.

To identify the ultimate frequency stability improvement that can be obtained with HC-PBGF as the delay element, we measured its net contribution to the overall OEO frequency drift. This required varying the temperature of the delay element whilst keeping the rest of the OEO loop (i.e. components in Part A, Fig. 1b) at a constant temperature. To do this, we placed the delay element in a temperature-controlled oven and enclosed the components in Part A in thermally-insulated foam box. Then we cycled the temperature within the oven between 26 °C and 36 °C (i.e. a 10 °C variation as shown in Fig. 3a) and measured the corresponding OEO carrier frequency drift.

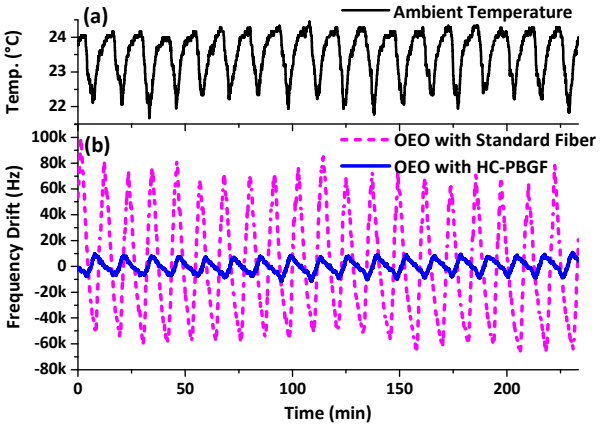

Fig. 2. (a) Ambient temperature variation measured at the OEO setup (by placing a thermistor in air between Part A and Part B). (b) Measured OEO frequency drift with all of its components exposed to ambient temperature variations.

As shown in Fig. 3b, for the 10 °C temperature change, the frequency of the standard fiber-based OEO changed by 810 kHz while the frequency of the HC-PBGF-based OEO changed just by 60 kHz. As mentioned earlier, the time delays induced by the two fibers were not identical (2.45 µs for standard fiber and 2.88 µs for HC-PBGF). Thus, we calculated OEO frequency drift per unit delay, which gave 331 GHz/s for standard fiber and 21 GHz/s for HC-PBGF. This shows that the HC-PBGF delay element was 15.8 times less temperature sensitive as compared to the standard fiber delay element.

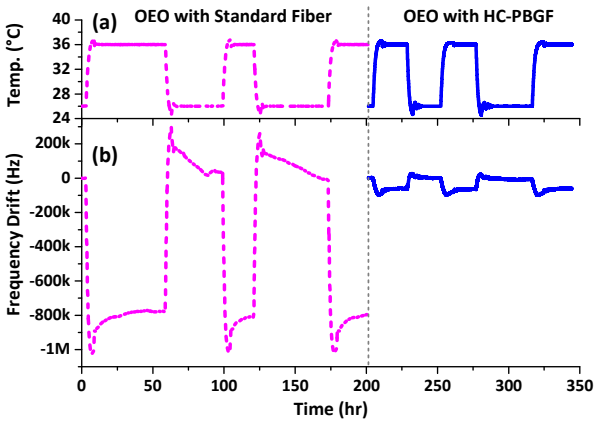

Fig. 3. (a) Temperature cycling of the OEO delay elements while keeping the rest of the OEO at a constant temperature, (b) Measured OEO frequency drift during temperature cycling.

Next we calculated the TCD of the two fibers used as the delay elements from the changes in the OEO loop delay ($\Delta\tau$), which can be expressed in terms of the frequency drift of the OEO(f_{drift}), carrier frequency of the OEO (f_{osc} = 10 GHz) and the free spectral range (FSR) of the OEO loop according to:

$$\Delta\tau = \tau_2 - \tau_1 = \frac{1}{FSR_2} - \frac{1}{FSR_1} \approx \frac{\Delta FSR}{FSR^2} = \frac{f_{drift}}{f_{osc} FSR} \qquad (2)$$

where subscripts 1, 2 are for two different temperatures, $\Delta FSR = FSR_1 - FSR_2$, and we assumed $FSR \approx FRS_1 \approx FSR_2$. Substituting this into Eq. 1 gives:

$$TCD = \frac{1}{\Delta TL}\left[\frac{f_{drift}}{f_{osc} FSR}\right] \qquad (3)$$

We measured the FSR from the RF output spectra (as there are always visible peaks in the RF spectrum corresponding to the cavity FSR) to be 320 kHz with HC-PBGF and 365 kHz with the standard fiber. Considering the f_{drift} values shown in Fig. 3, we calculated the TCD values to be 2.2 ps/km/K for the HC-PBGF delay element and 44.4 ps/km/K for the standard fiber delay element respectively. The calculated TCD of the HC-PBGF from our experiment is about 10% higher than that previously reported [13]. The TCD of standard fiber is also about 10% higher than the 40 ps/km/K reported in [18, 27]. We believe this discrepancy is due to the thermal expansion of the fiber spools used in our experiments.

Finally, we measured the close to carrier phase noise of the signals produced by the two OEOs (shown in Fig. 4) using the Photonic delay technique [28]. These measurements revealed that

the HC-PBGF-based OEO has higher phase noise at low offset frequencies as compared to the standard fiber-based OEO. Specifically, it is worse by 11 dB at a 1 kHz offset and 3 dB at a 10 kHz offset. This slight degradation is most likely due to the non-optimized signal launch conditions into/from the HC-PBGF and standard fiber pigtails and scattering inside the HC-PBGF, resulting in multi-path interference leading to increased intensity noise [21] that degrades the phase noise [22] as discussed earlier.

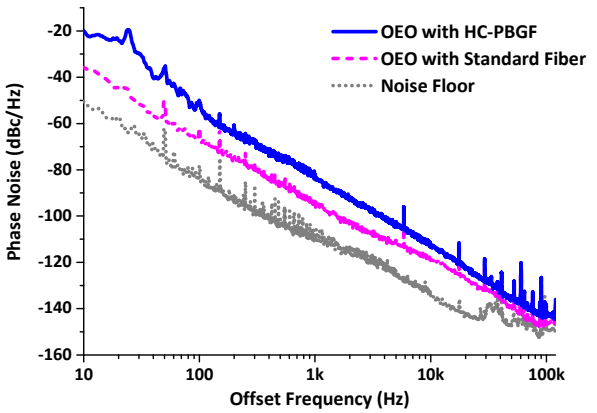

Fig. 4. Close to carrier phase noise properties of the OEO with the two delay elements.

In conclusion, we have demonstrated an OEO employing a 860 m long HC-PBGF fiber. Our experimental results show that up to 15.8 times better temperature stability can be achieved by replacing standard fiber with HC-PBGF. The phase noise of the HC-PBGF-based OEO was slightly degraded as compared to that based on standard fiber. We expect the current performance to be significantly improved by optimizing launch/output coupling (e.g., by using better-matched mode field adapters) into/from HC-PBGF and by utilizing lower-scattering-loss, higher modal-purity HC-PBGFs [29] which are expected to be available in the near future.

From the thermally-induced frequency drift of the OEO signal, we have evaluated the fibre thermal coeficient of delay (TCD) of HC-PBGF. Our result, 2.2 ps/km/K, is about 10% larger than that reported in Ref. [13] in which the measurement was performed on significantly shorter samples (less than 20 m) which were not spun on fiber spools, suggesting that this slight difference could be due to expansion of the spool.

In our future work, we plan to exploit a recently-published HC-PBGF that has zero TCD [30].

Funding. We acknowledge support from the UK Engineering and Physical Sciences Research Council (EPSRC) through grants EP/K003038/1, EP/I061196X and EP/I01196X/1 (The Photonic Hyperhighway) also from the EU H2020 Program through grant agreement 682724, 'Lightpipe'. F. Poletti and N.V. Wheeler gratefully acknowledge support from the Royal Society University Research Fellow scheme.

Acknowledgment. The data for this work is accessible through the University of Southampton Institutional Research Repository (DOI: 10.5258/SOTON/D0056).

References

1. L. Maleki, in *2012 European Frequency and Time Forum* (2012), p. 497.
2. X. Yao and L. Maleki, J. Opt. Soc. Am. B 13, 1725 (1996).
3. X. S. Yao and L. Maleki, IEEE J. Quant. Electron 36, 79 (2000).
4. I. Ozdur, D. Mandridis, N. Hoghooghi and P. J. Delfyett, J. Lightwave Technol. 28, 3100 (2010).
5. X. Yao and L. Maleki, Opt. Lett. 22, 1867 (1997).
6. W. Zhou and G. Blasche, IEEE Trans. Microw. Theory Tech. 53, 929 (2005).
7. A. B. Matsko, L. Maleki, A. A. Savchenkov and V. S. Ilchenko, J. Mod. Opt. 50, 2523 (2003).
8. K. Saleh, A. Bouchier, P. H. Merrer, O. Llopis and G. Cibiel, in *Proc. SPIE 7936, RF and Millimeter-Wave Photonics* (2011), paper 79360A.
9. D. Eliyahu, D. Seidel and L. Maleki, in *2008 IEEE International Frequency Control Symposium* (2008), p. 811.
10. D. Eliyahu, K. Sariri, J. Taylor and L. Maleki, in *Proc. SPIE 4998, Photonic Integrated Systems* (2003), p. 139.
11. D. Hou, X. P. Xie, Y. L. Zhang, J. T. Wu, Z. Y. Chen and J. Y. Zhao, Sci. Rep. 3, 3509 (2013).
12. Y. Zhang, D. Hou and J. Zhao J. Lightwave Technol. 32, 2408 (2014).
13. R. Slavík, G. Marra, E. N. Fokoua, N. Baddela, N. V. Wheeler, M. Petrovich, F. Poletti and D. J. Richardson, Sci. Rep. 5, 15447 (2015).
14. A. S. Daryoush, J. China Univ. Posts Telecommun. 16, 1 (2009).
15. G. Beck, L. Bigot, G. Bouwmans, A. Kudlinski, J. P. Vilcot and M. Douay, IEEE Photon. J 4, 789 (2012).
16. L. Zhang, V. Madhavan, R. P. Patel, A. K. Poddar, U. L. Rohde and A. S. Daryoush , in *IEEE MTT-S International Microwave and RF Conference* (2013), p. 1.
17. S. Blin, H. K. Kim, M. J. F. Digonnet and K. S. Gordon, J. Lightwave Technol. 25, 861 (2007).
18. H. Hartog, A. J. Conduit and D. N. Payne, Opt. Quant. Electron. 11, 265 (1979).
19. F. Poletti, N. V. Wheeler, M. N. Petrovich, N. Baddela, E. N. Fokoua, J. R. Hayes, D. R. Gray, Z. Li, R. Slavík and D. J. Richardson, Nat. Photon 7, 279 (2013).
20. P. Roberts, F. Couny, H. Sabert, B. Mangan, D. Williams, L. Farr, M. Mason, A. Tomlinson, T. Birks, J. Knight and P. Russel, Opt. Express 13, 236 (2005).
21. G. A. Cranch and G. A. Miller, Appl. Opt. 54, F8 (2015).
22. O. Okusaga, J. P. Cahill, A. Docherty, C. R. Menyuk, W. Zhou and G. M. Carter, Opt. Express 21, 22255 (2013).
23. N. Wheeler, M. Petrovich, R. Slavik, N. Baddela, E. Numkam Fokoua, J. Hayes, D. Gray, F. Poletti and D. Richardson, in *National Fiber Optic Engineers Conference, OSA Technical Digest* (Optical Society of America, 2012), paper PDP5A.2.
24. J. Wooler, S. Sandoghchi, D. Gray, F. Poletti, M. Petrovich, N. Wheeler, N. Baddela and D. Richardson, in *Workshop on Specialty Optical Fibers and their Applications* (Optical Society of America, 2013), paper W3.26.
25. Corning Incoperated, https://www.corning.com/media/worldwide/coc/documents/PI1463_07-14_English.pdf.
26. J. Švarný, in *2010 12th Biennial Baltic Electronics Conference (BEC2010)* (2010), p. 231.
27. M. Bousonville, M. K. Bock, M. Felber, T. Ladwig, T. Lamb, H. Schlarb, S. Schulz, C. Sydlo, S. Hunziker, P. Kownacki and S. Jablonski, in *Beam Instrumentation Workshop 2012 (BIW2012)* (2012), paper MOPG033.
28. E. Rubiola, E. Salik, S. Huang, N. Yu and L. Maleki, J. Opt. Soc. Am. B. 22, 987 (2005).
29. F. Poletti, Opt. Express 22, 23807 (2014).
30. E. Numkam Fokoua, M. N. Petrovich, . T. Bradley, F. Poletti, D. J. Richardson and R. Slavík, Optica (to be published)

FULL REFERENCES LIST

[1] L. Maleki, "The opto-electronic oscillator (OEO): Review and recent progress," in *2012 European Frequency and Time Forum (EFTF)* (2012), pp. 497-500

[2] X. S. Yao and L. Maleki, "Optoelectronic microwave oscillator," Journal of Optical Society of America B, vol. 13, no. 8, pp. 1725-1735 (1996).

[3] X. S. Yao and L. Maleki, "Multiloop Optoelectronic Oscillator," IEEE Journal of Quantum Electronics, vol. 36, no. 1, pp. 79-84 (2000).

[4] I. Ozdur, D. Mandridis, N. Hoghooghi and P. J. Delfyett, "Low Noise Optically Tunable Opto-Electronic Oscillator With Fabry–Perot Etalon," Journal of Lightwave Technology, vol. 28, no. 21, pp. 3100-3106 (2010).

[5] X. Yao and L. Maleki, "Dual microwave and optical oscillator," Optics Letters, vol. 22, no. 24, pp. 1867-1869 (1997).

[6] W. Zhou and G. Blasche, "Injection-locked dual opto-electronic oscillator with ultra-low phase noise and ultra-low spurious level," IEEE Transactions on Microwave Theory and Techniques, vol. 53, no. 3, pp. 929-933 (2005).

[7] A. B. Matsko, L. Maleki, A. A. Savchenkov and V. S. Ilchenko, "Whispering gallery mode based optoelectronic microwave oscillator," Journal of Modern Optics, vol. 50, no. 15-17, pp. 2523-2542 (2003).

[8] K. Saleh, A. Bouchier, P. H. Merrer, O. Llopis and G. Cibiel, "Fiber Ring Resonator Based Opto-Electronic Oscillator - Phase Noise Optimisation and Thermal Stability Study," Proc. SPIE 7936, RF and Millimeter-Wave Photonics, 79360A (2011).

[9] D. Eliyahu, D. Seidel and L. Maleki, "Phase noise of a high performance OEO and an ultra low noise floor cross-correlation microwave photonic homodyne system," in *2008 IEEE International Frequency Control Symposium* (2008) pp. 811-814.

[10] D. Eliyahu, K. Sariri, J. Taylor and L. Maleki, "Opto-Electronic Oscillator with Improved Phase Noise and Frequency Stability," Proc. SPIE 4998, Photonic Integrated Systems, 139 (2003).

[11] D. Hou, X. P. Xie, Y. L. Zhang, J. T. Wu, Z. Y. Chen and J. Y. Zhao, "Highly Stable Wideband Microwave Extraction by Synchronizing Widely Tunable Optoelectronic Oscillator with Optical Frequency Comb," Scientific reports, vol. 3, 3059 (2013).

[12] Y. Zhang, D. Hou and J. Zhao, "Long-Term Frequency Stabilization of an Optoelectronic Oscillator Using Phase-Locked Loop," Journal of Lightwave Technology, vol. 32, no. 13, pp. 2408-2414 (2014).

[13] R. Slavík, G. Marra, E. N. Fokoua, N. Baddela, N. V. Wheeler, M. Petrovich, F. Poletti and D. J. Richardson, "Ultralow thermal sensitivity of phase and propagation delay in hollow core optical fibres," Scientific Reports, vol. 5, 15447 (2015).

[14] A. S. Daryoush, "Thermal sensitivity of photonic crystal fibers in opto-electronic oscillators," The Journal of China Universities of Posts and Telecommunications, vol. 16, no. 4, pp. 1-6, (2009).

[15] G. Beck, L. Bigot, G. Bouwmans, A. Kudlinski, J. P. Vilcot and M. Douay, " Benefits of Photonic Bandgap Fibers for the Thermal Stabilization of Optoelectronic Oscillators," IEEE Photonics Journal, vol. 4, no. 3, pp. 789-794 (2012).

[16] L. Zhang, V. Madhavan, R. P. Patel, A. K. Poddar, U. L. Rohde and A. S. Daryoush , "Ultra low FM noise in passively temperature compensated microwave opto-electronic oscillators," in *IEEE MTT-S International Microwave and RF Conference* (2013) pp. 1-4.

[17] S. Blin, H. K. Kim, M. J. F. Digonnet and K. S. Gordon, "Reduced thermal sensitivity of a fiber-optic gyroscope using an air-core photonic-bandgap fiber," Journal of Lightwave Technology, vol. 25, no. 3, pp. 861-865, 2007

[18] A. H. Hartog, A. J. Conduit and D. N. Payne, "Variation of pulse delay with stress and temperature in jacketed and unjacketed optical fibres," Optical and Quantum Electronics, vol. 11, no. 3, pp. 265-273 (1979).

[19] F. Poletti, N. V. Wheeler, M. N. Petrovich, N. Baddela, E. N. Fokoua, J. R. Hayes, D. R. Gray, Z. Li, R. Slavík and D. J. Richardson, "Towards high-capacity fibre-optic communications at the speed of light in vacuum," Nature Photonics, vol. 7, no. 4, pp. 279-284 (2013).

[20] P. J. Roberts, F. Couny, H. Sabert, B. J. Mangan, D. P. Williams, L. Farr, M. W. Mason, A. Tomlinson, T. A. Birks, J. C. Knight and P. S. J. Russel, "Ultimate low loss of hollow-core photonic crystal fibres," Optics Express, vol. 13, no. 1, pp. 236-244 (2005).

[21] G. A. Cranch and G. A. Miller, "Coherent light transmission properties of commercial photonic crystal hollow core optical fiber," *Applied optics,* vol. 54, no. 31, pp. F8-F16, 2015.

[22] O. Okusaga, J. P. Cahill,, A. Docherty, C. R. Menyuk, W. Zhou and G. M. Carter, "Suppression of Rayleigh-scattering-induced noise in OEOs," *Optics Express,* vol. 21, no. 19, pp. 22255-22262, 2013

[23] N. Wheeler, M. Petrovich, R. Slavík, N. Baddela, E. Numkam Fokoua, J. Hayes, D. Gray, F. Poletti and D. Richardson, "Wide-bandwidth, low-loss, 19-cell hollow core photonic band gap fiber and its potential for low latency data transmission," in *National Fiber Optic Engineers Conference,* OSA Technical Digest (Optical Society of America, 2012), paper PDP5A.2.

[24] J. Wooler, S. Sandoghchi, D. Gray, F. Poletti, M. Petrovich, N. Wheeler, N. Baddela and D. Richardson, "Overcoming the challenges of splicing dissimilar diameter solid-core and hollow-core photonic band gap fibers," in *Workshop on Specialty Optical Fibers and their Applications,* (Optical Society of America, 2013), paper W3.26.

[25] Corning Incoperated, "Corning® SMF-28e+® Optical Fiber Product Information", https://www.corning.com/media/worldwide/coc/documents/PI1463_07-14_English.pdf

[26] J. Švarný, "Analysis of quadrature bias-point drift of Mach-Zehnder electro-optic modulator," in *2010 12th Biennial Baltic Electronics Conference (BEC2010)* (2010) pp 231-234.

[27] M. Bousonville, M. K. Bock, M. Felber, T. Ladwig, T. Lamb, H. Schlarb, S. Schulz, C. Sydlo, S. Hunziker, , P. Kownacki and S. Jablonski, "New phase stable optical fiber," in *Beam Instrumentation Workshop 2012 (BIW2012)* (2012), paper MOPG033

[28] E. Rubiola, E. Salik, S. Huang, N. Yu and L. Maleki, "Photonic-delay technique for phase-noise measurement of microwave oscillators," Journal of the Optical Society of America B, vol. 22, no. 5, pp. 987-997 (2005).

[29] F. Poletti, "Nested antiresonant nodeless hollow core fiber," Optics Express, vol. 22, no. 20, pp. 23807-23828 (2014).

[30] E. Numkam Fokoua, M. N. Petrovich, . T. Bradley, F. Poletti, D. J. Richardson and R. Slavík, "How to make the propagation time through an optical fiber fully insensitive to temperature variations," Optica (to be published)